Available online at www.sciencedirect.com
ScienceDirect
Journal of Molecular Catalysis A: Chemical 277 (2007) 171–179
JOURNAL OF MOLECULAR CATALYSIS A: CHEMICAL
www.elsevier.com/locate/molcata

The adsorption of saturated and unsaturated hydrocarbons on nanostructured zeolites (H-MOR and H-FAU): An ONIOM study

Piboon Pantu [a,b], Bundet Boekfa [a], Jumras Limtrakul [a,b,*]

[a] *Laboratory for Computational and Applied Chemistry, Department of Chemistry, Faculty of Science, Kasetsart University, Bangkok 10900, Thailand*
[b] *Center of Nanotechnology, Kasetsart University, Bangkok 10900, Thailand*

Received 13 June 2007; accepted 15 July 2007
Available online 26 July 2007

Abstract

The adsorption and interactions of light alkanes and alkenes on acidic zeolites (H-MOR and H-FAU) were theoretically studied using the ONIOM approach. With the basis set superposition error (BSSE) corrections, the ONIOM(MP2/6-31G(d,p):UFF//B3LYP/6-31G(d,p):UFF) adsorption energies of alkanes (ethane, propane, and *n*-butane) in H-FAU and H-MOR were in good agreement with the experimental measurements. For adsorption of alkenes in acidic zeolite which is not possible to experimentally measure, the adsorption energies were predicted to be −9.4, −11.3, and −12.5 kcal/mol for ethene, propene, and 1-butene in H-FAU, respectively and −10.1, −13.8, and −17.4 kcal/mol for ethene, propene, and 1-butene in H-MOR, respectively. It was found that the extended zeolitic framework covering the nanocavity was essential for describing the confinement effect of the zeolites and led to the differentiation of different types of zeolites. These results suggest that this ONIOM scheme is a practical method for investigating the adsorption of unsaturated and saturated hydrocarbons on these zeolites.

Keywords: Alkanes; Alkenes; Confinement effect; QM/MM; Zeolites

1. Introduction

Zeolite is one of the most important heterogeneous catalysts especially for the petrochemical industry. This microporous crystalline aluminosilicate contains strong Brønsted acidity and can facilitate many acid catalyzed reactions. Moreover, it contains a regular microporous structure with pore dimensions close to the sizes of the hydrocarbon molecules. Therefore, many petrochemical processes take advantage of the molecular shape selectivity of this type of catalyst, for instance in catalytic cracking, isomerization, and alkylation of hydrocarbons and aromatics. The zeolite pore size has been found to have significant effects on the adsorption and reaction of adsorbed molecules inside its nanostructured pores [1–4].

The term "confinement effect" [5,6] was proposed to explain the interactions between the zeolite framework and the adsorbed molecule which is confined within the pore of the zeolite. These interactions are mainly composed of dispersive van der Waals interactions. The confinement effects contribute to the remarkable sorption and catalytic properties of zeolites by stabilizing adsorbed molecules, intermediates, and reaction transition states. Derouane [7] has reconsidered the confinement effect to extend over all non-covalent interactions between the zeolite framework and the adsorbed molecule and, therefore, the zeolites may be considered as solid solvents when the size of adsorbate molecules and the zeolite pore dimensions are comparable.

The understanding and rational utilization of confinement effects will undoubtedly contribute to increasing the productivity, and selectivity of such chemical transformations [8–11]. Recently, experimental investigations in molecular details of structures and adsorption dynamics and interaction energies of hydrocarbons in zeolites have been reported [12–18]. It was found that the pore size of zeolites had strong effects on the geometries of adsorption sites, the structures of the adsorption complexes, and the adsorption energies. The adsorption of alkanes in zeolite is simply physisorption. The linear correlations of

* Corresponding author at: Laboratory for Computational and Applied Chemistry, Department of Chemistry, Faculty of Science, Kasetsart University, Bangkok 10900, Thailand. Fax: +66 2 562 5555x2119.
E-mail address: fscijrl@ku.ac.th (J. Limtrakul).

1381-1169/$ – see front matter © 2007 Elsevier B.V. All rights reserved.
doi:10.1016/j.molcata.2007.07.037

interaction energy (heat of adsorption) and the number of carbon atoms of *n*-alkanes have been found in various zeolites [19]. However, the adsorption of alkenes in acidic zeolites is complicated by the rapid reactions of oligomerization and isomerization at the Brønsted acid sites [17,18,20]. The heat of adsorption of alkenes cannot be experimentally measured because of these reactions. The most stable adsorbed structure for alkenes adsorption in zeolites is a π-adsorption complex where the π-electron of the double bond carbons forms a hydrogen bonding with the Brønsted acidic proton of the zeolite [20]. A less stable adsorption complex via interaction of the alkyl group of alkene and the Brønsted acid of the zeolite has also been reported [17,18]. It has also been proposed that the transition between these two adsorption structures may be important to the diffusion process of alkenes in microporous zeolites [17,18]. However, the molecular details of adsorption of alkanes and alkenes on zeolites with different pore sizes are still not completely understood.

Zeolites are microporous aluminosilicates with a large number of atoms in the unit cell. To obtain more manageable sizes for the ab-initio calculations, small clusters representing the catalytic active site have been studied in the past. However, this has meant that the essential confinement effect created by the part of the surrounding framework has been neglected. It is important, therefore, that the larger clusters which include such potential should be taken into consideration. To facilitate this, large quantum clusters and periodic calculations have been specifically developed. However, even though these calculations do provide accurate results, they are very expensive in terms of computational time and expense. This prohibits the use of accurate periodic structure calculations, that are computationally too expensive and even impractical to perform when very large zeolites are concerned. The recent development of hybrid methods, such as the embedded cluster or combined quantum mechanics/molecular mechanics (QM/MM) [21–26] methods, as well as the more general ONIOM (Our-own-N-layer Integrated molecular Orbital + molecular Mechanics) method [27,28] have brought a larger system within reach of obtaining accurate results at a more reasonable computational cost.

In this study, the adsorptions of linear alkanes and alkenes in different zeolites, (H-MOR and H-FAU), are examined and compared to understand the adsorption process and to address the confinement effect in these nanostructured materials. We employ the ONIOM method that takes advantage of the density functional theory, for the accurate treatment of the interactions of adsorbed molecules with the acid site of zeolite, and the universal force field (UFF) to account for the van der Waals interaction due to the confinement of the zeolite framework which has been found to be important for the adsorption and reaction in microporous zeolites [29–34]. Moreover, the single point energy calculations at the MP2 level of theory and the basis set superposition errors (BSSE) corrections are carried out to refine the interaction energy. This efficient scheme has demonstrated that it can yield adsorption energies close to the experimental measurements for the adsorption of alkanes and predict reasonable estimates for the adsorption of alkenes that cannot be measured experimentally.

2. Methods

The ONIOM approach was employed to model the different types of zeolites and their complexes with unsaturated and saturated hydrocarbons. For computational efficiency, only the small active region was treated accurately with the density functional theory method, while the contribution of interactions from the rest of the model was approximated by a less computationally demanding method. The B3LYP/6-31G(d,p) level of theory was applied for the 14T tetrahedral quantum cluster, which was considered to represent the active site of the zeolites. The 120T extended framework connecting the quantum region was treated with the universal force field (UFF) [35] to represent the van der Waals contributions from the interactions of adsorbed molecules with the zeolite pore structures. This force field has been previously reported to provide a good description of the short-range van der Waals interactions between the sorbate molecules and the zeolitic wall [32–34]. The models of 120 tetrahedral Si atoms of MOR and FAU were obtained from their crystal structures [36,37]. The FAU 14T quantum cluster was the 12-membered-ring window of 7.4 Å in diameter with one substituted aluminum atom (T2 position) and two terminal silyl groups. The attached 120T extended cluster was modeled with the UFF force field to represent the two connecting supercages (Fig. 1). Similarly, the MOR 14T quantum cluster (T1 position) was modeled to the 12-membered-ring (MR) window of the straight channel of 6.5 Å × 7.0 Å. The 120T extended cluster was modeled to cover an ample portion of the straight channel with the crossed 8 MR windows (2.8 Å × 5.7 Å) opening to the side pockets (Fig. 2).

All structure optimization was performed at the B3LYP/6-31G(d,p):UFF level of theory. In order to obtain more reliable interaction energies, the single point energy calculations at MP2/6-31G(d,p):UFF//B3LYP/6-31G(d,p):UFF and the basis set superposition errors (BSSE) corrections were carried out. The BSSE energy can be computed as:

$$\Delta E = E(\text{complex})^{\text{complex}} - E(\text{zeolite})^{\text{complex}} - E(\text{probe})^{\text{complex}}$$

The superscript means all separates component are calculated with the same absolute basis. All calculations were performed on the modern Linux workstation using the Gaussian03 code [38].

3. Results and discussion

3.1. Adsorption of light alkanes in H-FAU and H-MOR zeolites

ONIOM models for the H-FAU and H-MOR zeolites that are used in this study are illustrated in Figs. 1 and 2, respectively. The ONIOM models are subdivided into three parts. The inner part (catalytic center) is a fourteen-tetrahedral (14T) quantum cluster representing the active site. The second part is the 120T extended framework modeled by the Universal Force Field to account for the confinement effect of the surrounded zeolitic pore. The H-FAU model consists of a 14T quantum cluster which is the 12-membered-ring window of 7.4 Å in diameter with one substi-

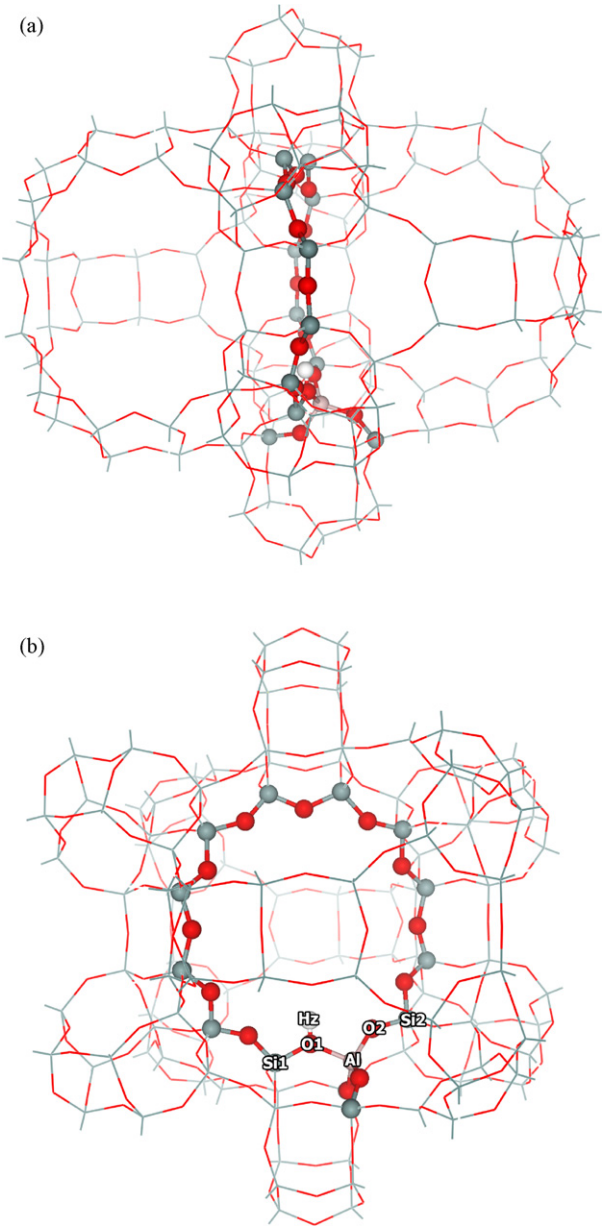

Fig. 1. The ONIOM model of 14T/120T cluster of H-FAU. (a) Side view shows the two supercages connected to the 14T quantum cluster and (b) front view shows the 12-membered-ring window connecting the two supercages. Atoms belonging to the 14T quantum region are drawn as spheres.

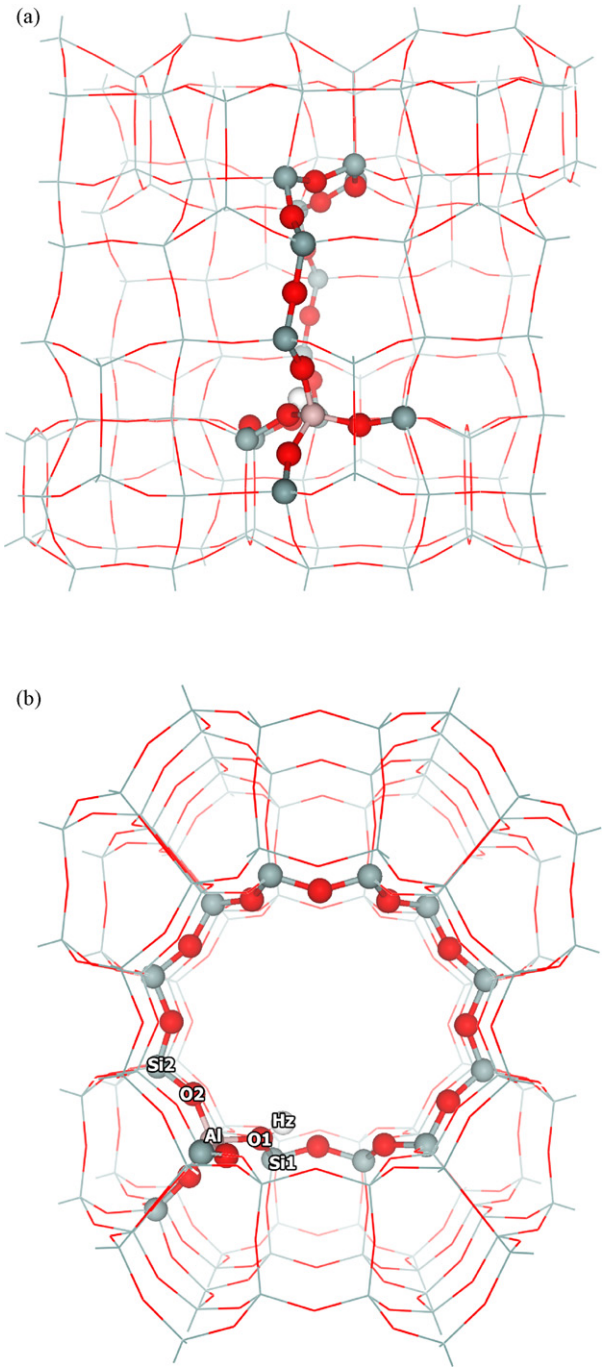

Fig. 2. The ONIOM model of 14T/120T cluster of H-MOR. (a) Side view of the 12-membered-ring straight channel and (b) front view shows the 12-membered-ring window of the straight channel. Atoms belonging to the 14T quantum region are drawn as spheres.

tuted aluminum atom and two terminal silyl groups. The attached 120T extended cluster is modeled with the UFF force field to represent the two connecting supercages (Fig. 1). The H-MOR 14T quantum cluster covers the 12-membered-ring (MR) window of the straight channel of 6.5 Å × 7.0 Å. The 120T extended cluster is modeled to cover an ample portion of the straight channel (Fig. 2).

The optimized structures of adsorption complexes of alkanes on H-FAU and H-MOR zeolites are illustrated in Figs. 3 and 4, respectively. Selected geometrical parameters of the complexes and their corresponding adsorption energies are listed in Table 1. The adsorption of alkanes in the microporous of zeolite occurs via weak interactions between the alkyl group and the Brønsted acid of the zeolite. Since the interactions are weak, there are only minute structural changes of the zeolite framework and the adsorbate upon the adsorption. The acidic OH bond distance is almost the same as in the isolated zeolite. The ethane adsorbs on the Brønsted acid by having an alkyl end of the molecule pointing to the acid site of the faujasite zeolite. The distance between the carbon atom of the adsorbed ethane and the zeolite proton (C1–Hz) is 2.32 Å. The adsorption energy is calculated to be −4.3 kcal/mol which agrees well with the experimentally mea-

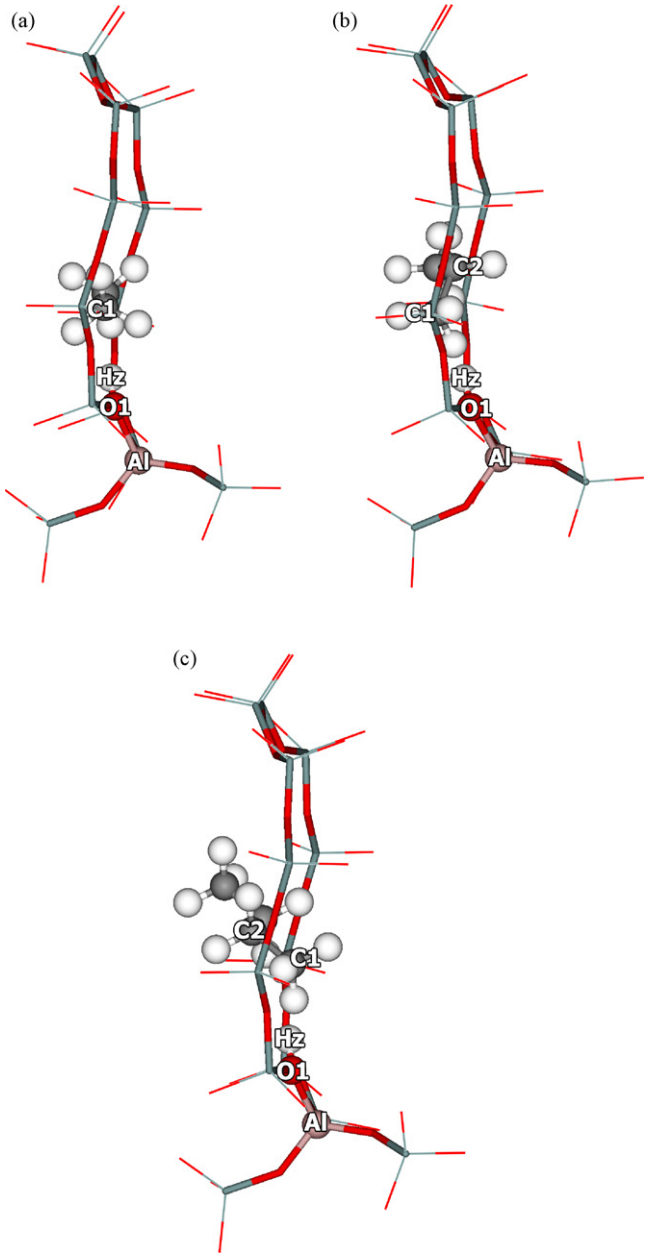

Fig. 3. The optimized structures of the adsorption complexes of (a) ethane, (b) propane, and (c) *n*-butane on H-FAU. Atoms on the adsorbed molecules and the Brønsted acid site are drawn as spheres and the extended framework is omitted.

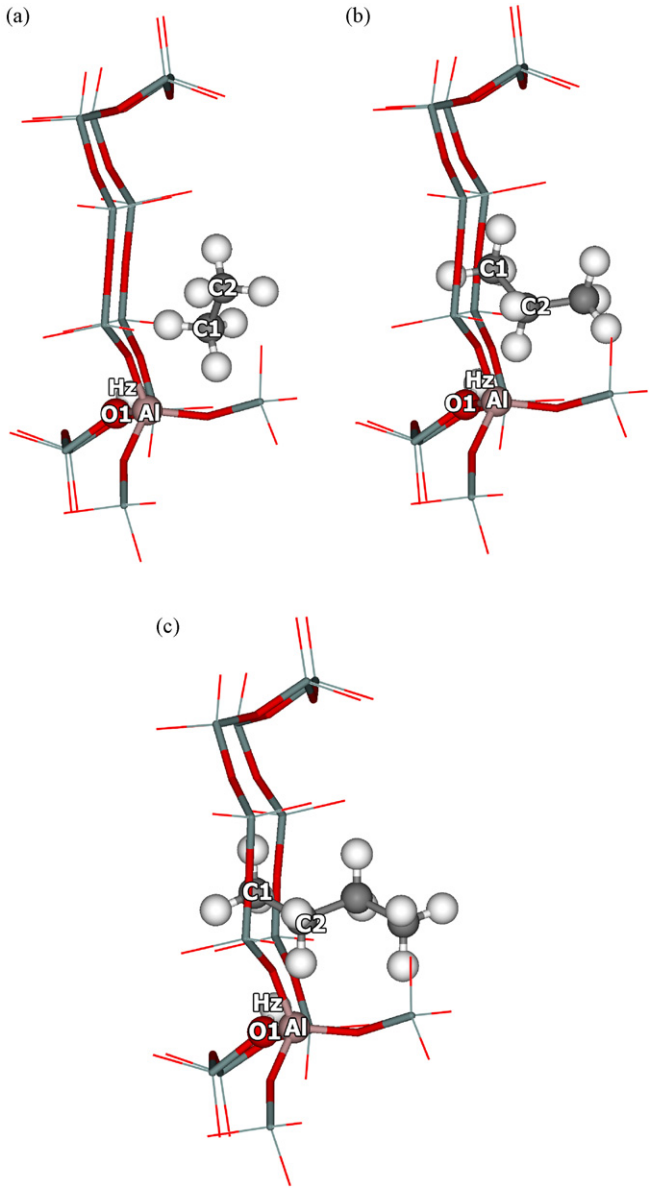

Fig. 4. The optimized structures of the adsorption complexes of (a) ethane, (b) propane, and (c) *n*-butane on H-MOR. Atoms on the adsorbed molecules and the Brønsted acid site are drawn as spheres and the extended framework is omitted.

sured value of −5.1 kcal/mol [39]. For propane and *n*-butane, two modes of adsorption are found, one via the terminal methyl (C1) and another via the internal methylene carbon (C2). In faujasite, it is found that the adsorption via the terminal methyl (C1) is slightly more stable with the C1–Hz distances of 2.33 and 2.37 Å for the adsorbed propane and *n*-butane, respectively. The energy differences between these two configurations are within 1 kcal/mol. The adsorption energies are calculated to be −5.8 and −7.1 kcal/mol, for propane and *n*-butane adsorption in H-FAU, respectively. The computed adsorption energies are in good agreement with the experimentally measured heats of adsorption of −6.4 and −8.1 kcal/mol for propane and *n*-butane, respectively [40,41].

In mordenite zeolite, the adsorption energies of these light alkanes are significantly larger since the pore confinement is more pronounced. The channel of H-FAU is 7.4 Å in diameter and, moreover, has two large supercages connected to it. While, the straight channel of H-MOR is elliptical with a dimension of 6.5 Å × 7.0 Å. The adsorption energies are calculated to be −8.2, −10.6, and −13.5 kcal/mol, for ethane, propane, and *n*-butane adsorption, respectively. The computed adsorption energies are also in good agreement with the measured heats of adsorption of −8.0, −9.8, −11.9 kcal/mol for ethane, propane, and *n*-butane adsorption in H-MOR, respectively [40–42].

In the ONIOM model, the interaction energies can be broken down to see the contribution of each layer. In this modeling scheme, the inner layer is calculated at the MP2 level of theory to represent the interaction between the adsorbate and the Brønsted

Table 1
The ONIOM(B3LYP/6-31G(d,p):UFF) optimized geometrical parameters and adsorption energies of ethane, propane, and *n*-butane in H-MOR and H-FAU

Parameters	H-MOR				H-FAU			
	Isolated	Ethane	Propane	*n*-Butane	Isolated	Ethane	Propane[a]	*n*-Butane[a]
Geometry								
Distance (Å)								
C1–C2[b]	1.53	1.53	1.53	1.53	1.53	1.53	1.54 (1.53)	1.53 (1.53)
C1–Hz		2.84	3.56	3.58		2.32	2.33 (3.33)	2.37 (3.49)
C2–Hz		3.68	2.56	2.67		3.57	3.70 (2.35)	3.60 (2.37)
O1–Hz	0.97	0.97	0.97	0.97	0.97	0.97	0.98 (0.98)	0.98 (0.98)
Al–O1	1.80	1.80	1.80	1.80	1.95	1.94	1.94 (1.94)	1.94 (1.94)
Si1–O1	1.68	1.68	1.68	1.68	1.71	1.70	1.70 (1.70)	1.70 (1.70)
Angle (°)								
O2–Al–O1	104.8	104.7	104.7	104.6	99.0	99.5	99.6 (99.7)	99.5 (99.8)
Si1–O1–Al	127.3	127.1	127.2	127.1	129.4	129.5	129.3 (129.3)	129.3 (129.3)
Energy (kcal/mol)								
B3LYP:UFF		−7.7	−9.8	−12.3		−4.6	−6.2 (−5.4)	−7.3 (−6.1)
MP2:UFF[c]		−8.2	−10.6	−13.5		−4.3	−5.8 (−5.5)	−7.1 (−6.4)
Experiment[d]		−8.0	−9.8	−11.9		−5.1	−6.4	−8.1

[a] Two adsorption structures were found. The parameters for the less stable adsorbed structure are in parenthesis.
[b] The C1–C2 distances of ethane, propane, and *n*-butane are 1.53 Å from the B3LYP/6-31G(d,p) calculations.
[c] Single point energy calculation at ONIOM(MP2/6-31G(d,p):UFF//B3LYP/6-31G(d,p):UFF) with the BSSE correction.
[d] From Refs. [13–15].

acid of the zeolite. The extended framework is modeled at a low level of theory by the UFF force field to represent the van der Waals interactions between the adsorbate and the zeolite pore wall. From the energy distribution (Table 2), one can see that the interaction of these light alkane molecules with the acid site of the zeolite is only a few kcal/mol, indicating that there is no strong interaction between the adsorbed alkanes and the acid site. The differences in the adsorption energies of these zeolites mainly arise from the low level contribution representing pore confinement. The van der Waals interactions contribute about 40% and 70% of the adsorption energies in H-FAU and H-MOR, respectively. It can be noticed that the van der Waals interactions increase with the sizes of the adsorbed molecules and have larger values in the smaller pore H-MOR than in the H-FAU. In H-MOR, the van der Waals interaction is clearly more important than the interaction with the acid site.

The computed adsorption energies that are in good agreement with the experimental measurements clearly demonstrate that the ONIOM model used in this work can represent interactions between the adsorbate molecules and the zeolites very well. The combination of the MP2 method at the active region embedded in the extended structure modeled by the UFF methods works well in representing electron correlation, and van der Waals interactions in the zeolite system.

3.2. Adsorption of light alkenes in H-FAU, H-MOR zeolites

The ONIOM models for the adsorption of alkenes on H-FAU and H-MOR zeolites are illustrated in Figs. 5 and 6, respectively. Selected geometrical parameters of the complexes and their corresponding adsorption energies are listed in Table 3. Alkene molecules are found to adsorb on the Brønsted acid of zeolites via the π-electrons of the double bond carbons as the most stable adsorption structure [20]. The changes in the structural parameters upon the adsorption are small. However, the changes are in accordance with Gutmann's rules [43], i.e. a lengthening of the O–H and C=C bonds and shortening of the Si–O and Al–O bonds. For all zeolites, the acidic O–H bond distance is slightly elongated by 0.01–0.03 Å and the C–C bond distance of ethene is slightly elongated by about 0.01 Å upon adsorption on H-

Table 2
The distribution of adsorption energy of light alkanes and alkenes on H-FAU and H-MOR calculated at embedded ONIOM(MP2/6-31G(d,p):UFF)//ONIOM(B3LYP/6-31G(d,p):UFF) with BSSE correction

	H-FAU			H-MOR		
	14T QM[a]	120T UFF[b]	Total	14T QM[a]	120T UFF[b]	Total
Ethane	−2.6	−1.7	−4.3	−2.0	−6.2	−8.2
Propane	−3.3	−2.5	−5.8	−3.2	−7.4	−10.6
n-Butane	−3.6	−3.5	−7.1	−3.6	−9.9	−13.5
Ethene	−7.3	−1.7	−9.0	−5.8	−4.2	−10.0
Propene	−8.4	−2.5	−10.9	−6.8	−6.8	−13.5
1-Butene	−8.9	−3.2	−12.1	−7.2	−9.9	−17.1

[a] Interaction energy from the 14T quantum cluster calculated at MP2/6-31G(d,p) with the BSSE correction.
[b] Interaction energy from the 120T extended framework modeled with the UFF.

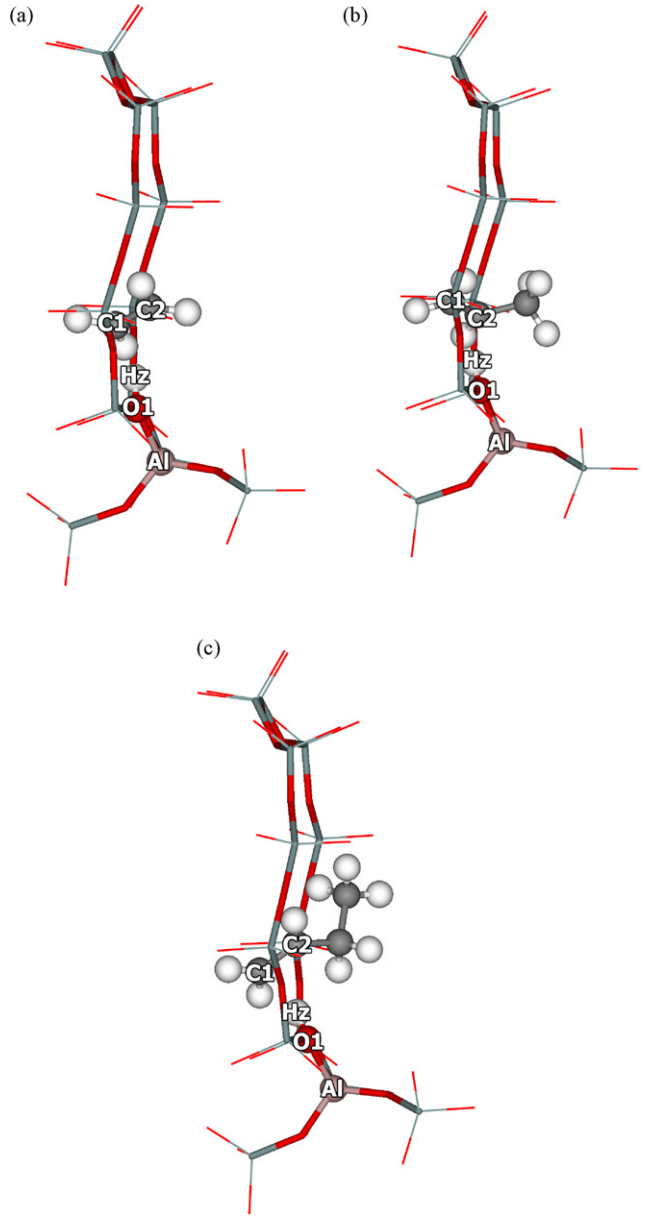

Fig. 5. The optimized structures of the adsorption complexes of (a) ethene, (b) propene and (c) 1-butene on H-FAU. Atoms on the adsorbed molecules and the Brønsted acid site are drawn as spheres and the extended framework is omitted.

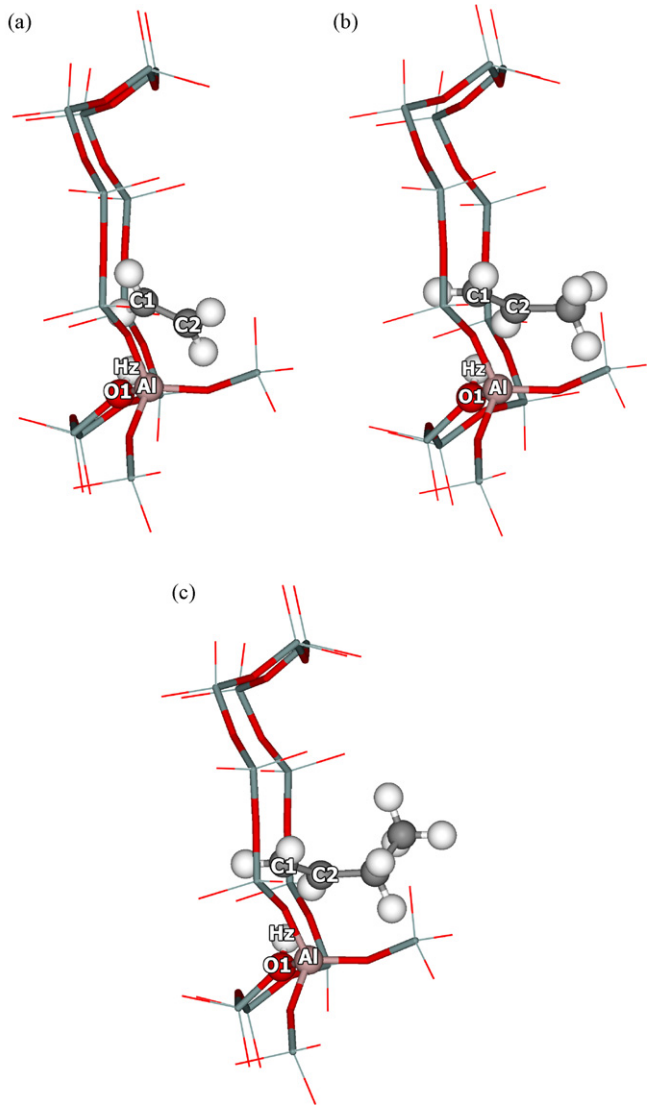

Fig. 6. The optimized structures of the adsorption complexes of (a) ethene, (b) propene and (c) 1-butene on H-MOR. Atoms on the adsorbed molecules and the Brønsted acid site are drawn as spheres and the extended framework is omitted.

FAU and H-MOR. The π-adsorption complexes of ethene on H-FAU and H-MOR have symmetrical structures with almost equal distances between C1–Hz and C2–Hz.

The calculated adsorption energy of ethene on H-FAU is −9.0 kcal/mol which is in excellent agreement with the experimental estimate of −9.1 kcal/mol [44]. The adsorption energy of ethene on H-MOR is −10.0 kcal/mol. The more exothermic adsorption energy in H-MOR is clearly due to the stronger confinement effect of the smaller pore dimension.

For larger unsaturated hydrocarbons, propene and 1-butene, the hydrogen bond complexes between the π-electrons of the double bond carbons and the acidic proton are not symmetrical. For instance, the C1–Hz and C2–Hz distances are 2.07 and 2.26 Å for propene adsorption on H-FAU. The more steric C2 carbon atom is located farther away from the zeolite framework. The predicted adsorption energies are −10.9 and −12.1 kcal/mol for propene and 1-butene adsorption on H-FAU, respectively and are −13.5 and −17.1 kcal/mol for propene and 1-butene adsorption on H-MOR, respectively. The adsorption energies in H-MOR are larger than in H-FAU by 1.0, 2.6, and 5.0 kcal/mol for the adsorption of ethene, propene, and 1-butene, respectively. These numbers demonstrate that the confinement effect is more pronounced when the size of the adsorbed molecule becomes larger.

A less stable adsorbed configuration was also considered. The optimized geometries of alkyl adsorption complexes of propene and 1-butene on H-FAU are presented in Fig. 7 and selected geometrical parameters and adsorption energies are listed in Table 4. In this adsorption configuration, the alkene molecules interact with the Brønsted acid of zeolites via the terminal alkyl group. The adsorption structures are similar to the adsorbed structures of the corresponding alkanes. The adsorption dis-

Table 3
The ONIOM(B3LYP/6-31G(d,p):UFF) optimized geometrical parameters and adsorption energies of ethene, propene and 1-butene in H-MOR and H-FAU

Parameters	H-MOR				H-FAU			
	Isolated	Ethene	Propene	1-Butene	Isolated	Ethene	Propene	1-Butene
Geometry								
Distance (Å)								
C1–C2[a]	1.33	1.34	1.34	1.34	1.33	1.34	1.34	1.34
C1–Hz		2.22	2.10	2.10		2.16	2.07	2.04
C2–Hz		2.23	2.30	2.35		2.17	2.26	2.22
O1–Hz	0.98	0.99	1.00	1.00	0.97	1.00	1.00	1.00
Al–O1	1.80	1.79	1.79	1.79	1.95	1.93	1.93	1.93
Si1–O1	1.68	1.67	1.67	1.67	1.71	1.70	1.70	1.70
Angle (°)								
O2–Al–O1	104.8	105.1	104.6	104.6	99.0	100.3	100.4	100.2
Si1–O1–Al	127.3	127.3	127.2	127.1	129.4	129.2	128.9	129.3
Energy (kcal/mol)								
B3LYP:UFF		−11.4	−14.5	−17.7		−10.9	−12.3	−13.2
MP2:UFF[b]		−10.0	−13.5	−17.1		−9.0	−10.9	−12.1
Experiment		–	–	–		−9.1[c]	–	–

[a] The C1–C2 distance of ethene, propene and 1-butene are 1.33 Å from the B3LYP/6-31G(d,p) calculations.
[b] Single point energy calculation at ONIOM(MP2/6-31G(d,p):UFF//B3LYP/6-31G(d,p):UFF) with the BSSE correction.
[c] From Ref. [17].

tances (C4–Hz) are 2.40 and 2.41 Å for adsorption of propene and 1-butene, respectively which are slightly longer than the adsorption distances of propane and butane on H-FAU by 0.07 and 0.04 Å, respectively. The alkyl interactions with the acid site are much weaker than that of the π-adsorption complex. The adsorption energies are calculated to be −5.6 and −6.6 kcal/mol for adsorption of propene and 1-butene, respectively, which are comparable to those of the corresponding alkane adsorption. Due to the weak alkyl interaction with the Brønsted acid of zeolites, this adsorption configuration will not contribute significantly to the adsorption energies of alkenes in the zeolites. However, this adsorption configuration may play a role in the diffusion of alkenes through the microporous of zeolite in which the molecules proceed through a series of adsorption and desorption on various sites along the zeolite pore channels [17,18].

The contributions of each layer in the computed ONIOM2 models are listed in Table 2. The π-electrons interactions with the Brønsted acid of the zeolites are stronger than the alkyl interactions. The interaction energies are in the range of 5.8–8.9 kcal/mol which are almost threefold higher than the alkyl interactions. Whereas, the van der Waals interactions are about the same for the adsorption of alkenes and alkanes with the

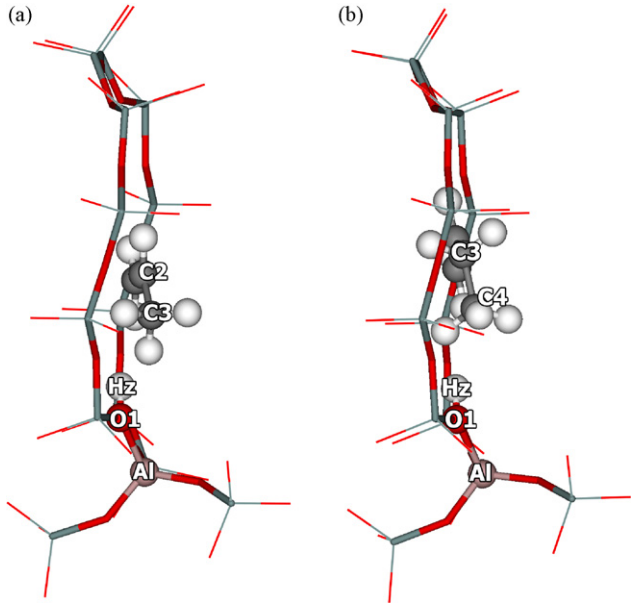

Fig. 7. The optimized structures of the adsorption complexes of (a) propene and (b) 1-butene on H-FAU via the terminal alkyl group. Atoms on the adsorbed molecules and the Brønsted acid site are drawn as spheres and the extended framework is omitted.

Table 4
The ONIOM(B3LYP/6-31G(d,p):UFF) optimized geometrical parameters and adsorption energies of propene and 1-butene in H-FAU via the terminal alkyl group

Parameters	H-FAU		
	Isolated	Propene	1-Butene
Geometry			
Distance (Å)			
C1–C2[a]	1.33	1.33	1.33
C–Hz[b]		2.40	2.41
O1–Hz	0.97	0.98	0.98
Al–O1	1.95	1.95	1.95
Si1–O1	1.71	1.70	1.71
Angle (°)			
O2–Al–O1	99.0	99.7	99.8
Si1–O1–Al	129.4	129.3	129.1
Energy (kcal/mol)			
B3LYP:UFF		−5.7	−6.6
MP2:UFF[c]		−5.6	−6.6

[a] The C1–C2 distance of propene and 1-butene are 1.33 Å from the B3LYP/6-31G(d,p) calculations.
[b] Distance from the terminal carbon (C3, C4 for propene and 1-butene, respectively) to the Brønsted acid proton.
[c] Single point energy calculation at ONIOM(MP2/6-31G(d,p):UFF//B3LYP/6-31G(d,p):UFF) with the BSSE correction.

same carbon number. The van der Waals interactions contribute about 20% and 50% of the adsorption energies of the alkenes in H-FAU and H-MOR, respectively.

There is no experimental data for adsorption energies of alkenes on proton forms of zeolites which is due to the facile reactions of isomerization and oligomerization of alkenes over acidic zeolites [17,18,20]. The only available adsorption energy is for small ethene in H-FAU zeolite. Our predicted value of −9.0 kcal/mol is in excellent agreement with the experimental estimate of −9.1 kcal/mol obtained by Cant and Hall [44], indicating that this ONIOM model can accurately compute the π-electron interaction with Brønsted acid of the zeolites. Moreover, the model has demonstrated its accuracy in describing the confinement effect of the zeolites by giving adsorption energies of alkanes that are in good agreement the experimental measurements. Therefore, our predicted adsorption energies of propene and 1-butene should be reasonable estimates. These results suggest that this embedded ONIOM scheme provides a practical method for investigating the adsorption of unsaturated and saturated hydrocarbons on zeolites.

4. Conclusions

The adsorption of light alkanes and alkenes were studied by using the embedded ONIOM approach. The embedded ONIOM2 calculations gave accurate adsorption energies for the adsorption of ethane, propane, and *n*-butane in H-FAU and H-MOR that were in good agreement with the experimental measurements. For adsorption of alkenes in acidic zeolite which is not possible to experimentally measured, the adsorption energies were predicted to be −9.0, −10.9, −12.1 kcal/mol for ethene, propene, and 1-butene in H-FAU, respectively and −10.0, −13.5, −17.1 kcal/mol for ethene, propene, and 1-butene in H-MOR, respectively. The ONIOM model used in this study can correctly describe the confinement effect of zeolite. The quantum cluster calculation can accurately compute interactions of the adsorbate with the acid site but cannot cover the van der Waals interactions with the zeolite walls. The extended zeolitic framework that was modeled by the UFF force field was found to be essential for describing the confinement effect of the zeolite and led to the differentiation of different types of zeolites.

Acknowledgements

This work was supported in part by grants from the Thailand Research Fund (to PP and JL) and the Kasetsart University Research and Development Institute (KURDI), the National Nanotechnology Center (NANOTEC center of Excellence and CNC Consortium) and the Commission on Higher Education, Ministry of Education under Postgraduate Education and Research Programs in Petroleum and Petrochemicals, and Advanced Materials.

References

[1] J. Wei, Ind. Eng. Chem. Res. 33 (1994) 2467.
[2] E.G. Derouane, C.D. Chang, Micropor. Mesopor. Mater. 35/36 (2000) 425.
[3] M. Boronat, C.M. Zicovich-Wilson, P. Viruela, A. Corma, J. Phys. Chem. B 105 (2001) 11169.
[4] J.A. van Bokhoven, B.A. Williams, W. Ji, D.C. Koningsberger, H.H. Kung, J.T. Miller, J. Catal. 224 (2004) 50.
[5] E.G. Derouane, J.M. Andre, A.A. Lucus, J. Catal. 110 (1988) 58.
[6] C.M. Zicovich-Wilson, A. Corma, P. Viruela, J. Phys. Chem. 98 (1994) 10863.
[7] E.G. Derouane, J. Mol. Catal. A: Chem. 134 (1998) 29.
[8] A. Corma, H. García, G. Sastre, P.M. Viruela, J. Phys. Chem. B 101 (1997) 4575.
[9] S.M. Babitz, B.A. Williams, J.T. Miller, R.Q. Snurr, W.O. Haag, H.H. Kung, Appl. Catal. A 179 (1999) 71.
[10] D. Dubbeldam, S. Calero, T.L.M. Maesen, B. Smit, Angew. Chem. Int. Ed. 42 (2003) 3624.
[11] T.L.M. Maesen, E. Beerdsen, S. Calero, D. Dubbeldam, B. Smit, J. Catal. 237 (2006) 278.
[12] J.A.Z. Pieterse, S. Veefkind-Reyes, K. Seshan, J.A. Lercher, J. Phys. Chem. B 104 (2000) 5715.
[13] L. Yang, K. Trafford, O. Kresnawahjuesa, J. Sepa, R.J. Gorte, D. White, J. Phys. Chem. B 105 (2001) 1935.
[14] D. Schuring, A.O. Koriabkina, A.M. de Jong, B. Smit, R.A. van Santen, J. Phys. Chem. B 105 (2001) 7690.
[15] F. Tielens, J.F.M. Denayer, I. Daems, G.V. Baron, W.J. Mortier, P. Geerlings, J. Phys. Chem. B 107 (2003) 11065.
[16] A. Zecchina, G. Spoto, S. Bordiga, Phys. Chem. Chem. Phys. 7 (2005) 1627.
[17] J.N. Kondo, K. Domen, J. Mol. Catal. A: Chem. 199 (2003) 27.
[18] E. Yoda, J.N. Kondo, K. Domen, J. Phys. Chem. B 109 (2005) 1464.
[19] E.G. Derouane, J.M. Andre, A.A. Lucas, J. Catal. 110 (1998) 58.
[20] G. Spoto, S. Bordiga, G. Ricchiardi, D. Scarano, A. Zecchina, E. Borello, J. Chem. Soc., Faraday Trans. 90 (1994) 2827.
[21] M. Brändle, J. Sauer, J. Am. Chem. Soc. 120 (1998) 1556.
[22] S.P. Greatbanks, I.H. Hillier, N.A. Burton, P. Sherwood, J. Chem. Phys. 105 (1996) 3770.
[23] J. Limtrakul, S. Jungsuttiwong, P. Khongpracha, J. Mol. Struct. 525 (2000) 153.
[24] P. Treesukol, J.P. Lewis, J. Limtrakul, T.N. Truong, Chem. Phys. Lett. 350 (2001) 128.
[25] R.Z. Khaliullin, A.T. Bell, V.B. Kazansky, J. Phys. Chem. A 105 (2001) 10454.
[26] I.H. Hillier, Theochem 463 (1999) 45.
[27] S. Dapprich, I. Komiromi, K.S. Byun, K. Morokuma, M.J. Frisch, Theochem 461/462 (1999) 1.
[28] M. Svensson, S. Humbel, R.D.J. Froese, T. Matsubara, S. Sieber, K. Morokuma, J. Phys. Chem. 100 (1996) 19357.
[29] P.E. Sinclair, A. de Vries, P. Sherwood, C.R.A. Catlow, R.A. van Santen, J. Chem. Soc., Faraday Trans. 94 (1998) 3401.
[30] K. Sillar, P. Burk, Theochem 589 (2002) 281.
[31] X. Solans-Monfort, M. Sodupe, V. Branchadell, J. Sauer, R. Orlando, P. Ugliengo, J. Phys. Chem. B 109 (2005) 3539.
[32] S. Kasuriya, S. Namuangruk, P. Treesukol, M. Tirtowidjojo, J. Limtrakul, J. Catal. 219 (2003) 320.
[33] S. Namuangruk, P. Pantu, J. Limtrakul, ChemPhysChem 6 (2005) 1333.
[34] S. Namuangruk, P. Khongpracha, P. Pantu, J. Limtrakul, J. Phys. Chem. B 110 (2006) 25950.
[35] A.K. Rappe, C.J. Casewit, K.S. Colwell, W.A. Goddard, W.M. Skiff, J. Am. Chem. Soc. 114 (1992) 10024.
[36] A. Alberti, P. Davoli, G.Z. Vezzalini, Kristallography 175 (1986) 249.
[37] D.H. Olson, E. Dempsey, J. Catal. 13 (1969) 221.
[38] M.J. Frisch, G.W. Trucks, H.B. Schlegel, G.E. Scuseria, M.A. Robb, J.R. Cheeseman, J.A. Montgomery Jr., T. Vreven, K.N. Kudin, J.C. Burant, J.M. Millam, S.S. Iyengar, J. Tomasi, V. Barone, B. Mennucci, M. Cossi, G. Scalmani, N. Rega, G.A. Petersson, H. Nakatsuji, M. Hada, M. Ehara, K. Toyota, R. Fukuda, J. Hasegawa, M. Ishida, T. Nakajima, Y. Honda, O. Kitao, H. Nakai, M. Klene, X. Li, J.E. Knox, H.P. Hratchian, J.B. Cross, V. Bakken, C. Adamo, J. Jaramillo, R. Gomperts, R.E. Stratmann, O. Yazyev, A.J. Austin, R. Cammi, C. Pomelli, J.W. Ochterski, P.Y. Ayala,

K. Morokuma, G.A. Voth, P. Salvador, J.J. Dannenberg, V.G. Zakrzewski, S. Dapprich, A.D. Daniels, M.C. Strain, O. Farkas, D.K. Malick, A.D. Rabuck, K. Raghavachari, J.B. Foresman, J.V. Ortiz, Q. Cui, A.G. Baboul, S. Clifford, J. Cioslowski, B.B. Stefanov, G. Liu, A. Liashenko, P. Piskorz, I. Komaromi, R.L. Martin, D.J. Fox, T. Keith, M.A. Al-Laham, C.Y. Peng, A. Nanayakkara, M. Challacombe, P.M.W. Gill, B. Johnson, W. Chen, M.W. Wong, C. Gonzalez, J.A. Pople, Gaussian 03, Gaussian, Inc., Wallingford, CT, 2004.

[39] H. Stach, U. Lohse, H. Thamm, W. Schirmer, Zeolites 6 (1986) 74.
[40] F. Eder, M. Stockenhuber, J.A. Lercher, J. Phys. Chem. B 101 (1997) 5414.
[41] F. Eder, J.A. Lercher, Zeolites 18 (1997) 75.
[42] G.D. Mayorga, D.L. Peterson, J. Phys. Chem. 76 (1972) 1647.
[43] V. Gutmann, The Donor-Acceptor Approach to Molecular Interaction, Plenum Press, New York, 1978.
[44] N.W. Cant, W.K. Hall, J. Catal. 25 (1972) 161.